Integrative and Comparative Biology
Integrative and Comparative Biology, volume 59, number 4, pp. 777–785
doi:10.1093/icb/icz106
Society for Integrative and Comparative Biology

SYMPOSIUM

“Beyond Primary Sequence”—Proteomic Data Reveal Complex Toxins in Cnidarian Venoms

Adrian Jaimes-Becerra,[*] Ranko Gacesa,[†] Liam B. Doonan,[‡] Ashlie Hartigan,[§] Antonio C. Marques,[*] Beth Okamura[§] and Paul F. Long[1,*,‡,¶]

[*]Departamento de Zoologia, Instituto de Biociências, Universidade de São Paulo, Rua Matão, Trav. 14, 101, São Paulo 05508-090, Brazil; [†]Department of Gastroenterology and Hepatology, University Medical Centre Groningen, Postbus 30.001, Groningen 9700 RB, The Netherlands; [‡]Faculty of Life Sciences and Medicine, King’s College London, 150 Stamford Street, London SE1 9NH, UK; [§]Department of Life Sciences, Natural History Museum, Cromwell Road, London SW7 5BD, UK; [¶]Faculdade de Ciências Farmacêuticas, Universidade de São Paulo, Av. Prof. Lineu Prestes, 580, B16, São Paulo 05508-000, Brazil

The first two authors contributed equally to this work.

From the symposium “Chemical responses to the biotic and abiotic environment by early diverging metazoans revealed in the post-genomic age” presented at the annual meeting of the Society for Integrative and Comparative Biology, January 3–7, 2019 at Tampa, Florida.

[1]E-mail: paul.long@kcl.ac.uk

Synopsis Venomous animals can deploy toxins for both predation and defense. These dual functions of toxins might be expected to promote the evolution of new venoms and alteration of their composition. Cnidarians are the most ancient venomous animals but our present understanding of their venom diversity is compromised by poor taxon sampling. New proteomic data were therefore generated to characterize toxins in venoms of a staurozoan, a hydrozoan, and an anthozoan. We then used a novel clustering approach to compare venom diversity in cnidarians to other venomous animals. Comparison of the presence or absence of 32 toxin protein families indicated venom composition did not vary widely among the 11 cnidarian species studied. Unsupervised clustering of toxin peptide sequences suggested that toxin composition of cnidarian venoms is just as complex as that in many venomous bilaterians, including marine snakes. The adaptive significance of maintaining a complex and relatively invariant venom remains unclear. Future study of cnidarian venom diversity, venom variation with nematocyst types and in different body regions are required to better understand venom evolution.

Introduction

Venoms are a complex mixture of organic and inorganic compounds that are delivered by inflicting a wound. Peptides and proteins are the most prevalent and deadliest constituents of venoms and are colloquially referred to as toxins (Nelsen et al. 2014). The toxin complement of venom has been suggested to reflect its function. For instance, defensive venoms of teleost fish and insects, whose main action is often to cause an extreme and immediate pain, tend to be comparatively simple in composition (Church and Hodgson 2002; Peiren et al. 2005; De Graaf et al. 2009). In contrast, predator venoms elicit wide ranging physiological effects and are more complex and variable in composition (Fry et al. 2009).

Cnidarians are probably the most ancient group of extant venomous animals. Their unique mechanism of venom delivery involves nematocysts—intracellular organelles produced within “stinging cells” (nematocytes) that are strategically positioned in the ectoderm and endoderm. Approximately 30 different types of nematocysts are known, and species are usually characterized by two to six types (Weill 1934; Östman 2000). Characterization of venom toxins using new and increasingly affordable sequencing platforms, particularly for high-throughput proteomics,

Advance Access publication July 8, 2019

has significantly expanded our knowledge of venoms. The first use of tandem mass spectrometry for high-throughput characterization of cnidarian material (*Symbiodinium* sp. endosymbionts in the coral *Stylophora pistillata*) identified toxins of contaminating coral nematocysts. The study provided evidence for an unexpectedly high sequence homology between cnidarian and vertebrate toxins (Weston et al. 2012). A subsequent proteomics study of nematocyst extracts of the hydrozoan *Olindias sambaquiensis* confirmed this high homology (Weston et al. 2013), and led to a reinvigoration of research into the nature and provenance of venoms in these early diverging metazoans (Starcevic and Long 2013).

The major toxic activities of venomous bilaterians involve enzymatic, neurotoxic, and cytolytic actions (Šuput 2009; Badré 2014; Mariottini et al. 2015). Data from recent proteomic and transcriptomic studies collectively suggest that genes encoding toxins with predominantly cytolytic and neurotoxic activities were also recruited into the venom of cnidarian precursors (Balasubramanian et al. 2012; Li et al. 2014, 2016; Brinkman et al. 2015; Macrander et al. 2015; Rachamim et al. 2015; Huang et al. 2016; Ponce et al. 2016; Madio et al. 2017). Subsequent divergence entailed lineage-specific functional recruitment of certain toxin protein families, with cytolysins diversifying in Medusozoa and neurotoxins in Anthozoa (Brinkman et al. 2015; Rachamim et al. 2015; Jaimes-Becerra et al. 2017). Pore-forming toxins appear to be ubiquitous in anthozoans and medusozoans, the most representative examples being the actinoporins, Cry-like jellyfish toxins, aerolysin-like toxins, and MACPF/CDC toxins (Podobnik and Anderluh 2017). However, limited taxon sampling may bias understanding of venom evolution in cnidarians, and it is unclear how cnidarian toxin diversity compares with that of other venomous animals. A broader sampling of toxins across major cnidarian lineages is required to enable more meaningful insights into these issues. The aims of this study were to: 1) gain the first insights into venom of a staurozoan (*Haliclystus antarcticus*); 2) to broaden taxon sampling by characterizing venoms of a hydrozoan (*Ectopleura crocea*) and an anthozoan (*Tubastraea coccinea*), and 3) to compare toxin diversity and venom evolution in cnidarians and other animals by employing unsupervised clustering of pair-wise sequence similarity data using our new and previously acquired data.

Materials and methods

Material

All animals were collected in accordance with SISBIO license 15031-2. Medusa stages of *H. antarcticus* were collected by bottom shrimp trawls at 19 m deep along Hall Peninsula on the southeast coast of Snow Island in the South Shetland Islands, Antarctica (−62°46′59.99″ S −61°22′59.99″ W). Eight clusters of secondary tentacles of approximately 3 mm in length were excised from one individual and lyophilized. Proteomic determination of the tentacle toxin content was conducted because recovery of sufficient nematocyst material was not possible. *E. crocea* and *T. coccinea* material was collected by hand from colonies on mooring pontoons at the Yacht Club de Ilhabela in Brazil (23°46′20″ S, 45°21′20″ W). Approximately 50 hydranths were collected from a single colony of *E. crocea* and some 20 tentacles were cut from polyps of from a single colony of *T. coccinea*. Nematocysts were isolated from the dissected tissues of both animals using previously described methods (Weston et al. 2013).

Protein extraction

Lyophilized tentacle tissue was homogenized in micro-centrifuge tubes using a micro-tube pestle in an equivalent weight of ice cold lysis buffer consisting of 100 mM Tris–HCl pH 7.5, 1% (w/v) Triton X-100, 0.2% (w/v) SDS, 300 mM NaCl, 0.2% (w/v) sodium deoxycholate, 2× protease inhibitors, and 2× phosphatase inhibitors (Halt Cocktail, Thermo Fisher Scientific Inc., Hemel Hempstead, UK). Samples were homogenized for 1 min, and then incubated on ice for 4 min. This was repeated over the course of 1 h. The homogenate was centrifuged at 14,000× g for 20 min at 4°C. The supernatant was transferred to a fresh tube. An equivalent volume of lysis buffer was then added to the collected pellet, and the pellet was re-homogenized for 30 min. The homogenate was again centrifuged at 14,000 ×g for 20 min at 4°C. The two supernatants containing solubilized proteins were then combined and the proteins precipitated using a mixture of methanol, chloroform, and water. The protein pellet was collected by centrifugation and dried to remove excess methanol. The pellet was solubilized in a buffer consisting of 100 mM triethylammonium bicarbonate, 0.1% (w/v) SDS, and 10 mM Tris (2-carboxyethyl) phosphine hydrochloride. The pellet was disrupted using a water bath sonicator and proteins allowed to solubilize at room temperature. An aliquot of sample was taken to measure protein concentration using the Bradford assay.

Protein preparation

A total of 300 µg of protein extract was reduced by adding 5 µL of 9 mM TCEP (Tris(2-carboxyethyl)-phosphine hydrochloride) in 50 mM TEAB and incubated for 1 h at 55°C. Iodoacetamide was then added to give a final concentration of 18 mM and the mixture then incubated for 30 min protected from light to alkylate proteins. In-solution digestion was performed by adding trypsin at a weight ratio of 1:40 trypsin to protein, and then incubating the reaction mixture overnight at 37°C. Trifluoroacetic acid was added to the sample to give a final concentration of 0.1% (v/v). The sample was desalted by solid phase extraction using an Oasis HLB 1cc, 30 mg extraction cartridge (Waters Ltd., Hertfordshire, UK). Eluted peptides were lyophilized and then reconstituted in OFFGEL peptide solubilization buffer containing 1.2% (v/v) IPG buffer pH 3–10 (GE Healthcare, Amersham, UK). Peptides were fractionated into 12 fractions using a 3100 OFFGEL Fractionator (Agilent Technologies, Cheadle, UK) and a 13 cm Immobiline DryStrip, pH 3–10 (GE Healthcare) for a total run time of 20 kV h. Fractionated peptides were collected and trifluoroacetic acid was added to each fraction to give a final concentration of 0.1% (v/v). Fractions were desalted for a final time with Zip Tip c18 (Merck Millipore Ltd, Watford, UK) and lyophilized.

LC/MS

Fractionated peptides were reconstituted in a buffer consisting of 2% (v/v) acetonitrile and 0.1% (v/v) formic acid. One-third of each fraction was loaded for tandem mass spectrometry analysis. Chromatography was performed with an EASY NanoLC (Thermo Fisher Scientific). Peptides were resolved by reverse phase chromatography on a 50 cm length, 75 µm internal diameter Acclaim PepMap RSLC column (Thermo Fisher Scientific) using a 120 min, linear gradient ranging from 10% (v/v) to 80% (v/v) acetonitrile in 0.1% (v/v) formic acid delivered at a flow-rate of 300 nL/min. Eluted peptides were ionized by electrospray ionization and analyzed using a collision induced dissociation (CID) method on an Orbitrap Fusion (Thermo Fisher Scientific) operating under Xcalibur v2.2. Fractions were analyzed sequentially with a 20 min column-wash between each fraction.

Data analysis

Mass spectrometry rawfiles were processed for database spectral matching using Proteome Discoverer v1.4 (Thermo Fisher Scientific). Mascot software v2.2 (Matrix Science Ltd., London, UK) was used as the search algorithm specifying the use of trypsin as the digestion enzyme allowing up to three missed cleavages, with oxidized-methionine as a variable modification and carbamidomethylated-cysteine as a fixed modification. A precursor ion mass tolerance of 20 ppm and a fragment ion mass tolerance of 0.8 Da were set. All fractions were analyzed using Multidimensional Protein Identification Technology (MudPIT). Spectra were searched against well annotated putative animal toxins downloaded from UniProtKB/SwissProt-ToxProt (Jungo et al. 2012). The dataset was also searched against our custom-built database of cnidarian toxins absent in UniProtKB/SwissProt-ToxProt. All duplicate entries with identical sequence or sequence identifier were removed. Mascot search results were uploaded to Scaffold Proteomics Data Viewer (www.proteome-software.com) and spectra were manually validated for unbroken series of over-lapping b-type and y-type sequence-specific fragment ions with neutral losses consistent with the sequence.

The peptide fragments from each validated spectrum used to assign annotation were taken as the input for a unique stringent nine step process to validate the annotation using a machine learning tool called "ToxClassifier" that was developed to exclude proteins with possible non-toxic physiological functions (Gacesa et al. 2016).

A Venn diagram was constructed using InteractiVenn (Heberle et al. 2015) from a matrix of presence and absence of putative toxin protein families, together with eight previously published venom proteomes (Jaimes-Becerra et al. 2017), to reflect total similarity. The previously published venom proteomes were selected to ensure identical bioinformatics approaches for annotating unique MS/MS events were employed across studies. The toxins from the combined data set were assigned to venom toxin protein families using established KEGG ontology. Data were coded in a matrix as presence (1) or absence (0) of each toxin protein family in each species (Supplementary File S1).

Comparative venom profiles

To compare the toxin diversity of cnidarian venoms with toxin diversity of higher animals we adapted an unsupervised clustering method based on pairwise sequence alignment, similar to the algorithm implemented in the CLANS tool for visualization of proteins (Frickey and Lupas 2004). This approach was adopted in order to deal with problems of aligning multiple input sequences. Generating such an alignment for the ~7000 toxin proteins is unfeasible due to computational costs and sequence divergence between different venom families (Frickey and Lupas 2004). Therefore, the sequence similarity of each pair of 6812 animal venom toxin proteins (downloaded from UniProtKB/Swiss-Prot Tox-Prot database of animal venoms) (Jungo et al. 2012) was calculated as the *e*-value of a pairwise blastp search (Camacho et al. 2009) to generate a similarity matrix of toxins. The *t*-distributed stochastic neighbor embedding (*t*-SNE) clustering (van der Maaten and Hinton 2008) implemented in Rtsne package (v.0.13) for statistical programming language R (v.3.4.3) was then applied to the similarity matrix to cluster the data and allow visualization in two dimensions.

Results and discussion

Three new venom toxin proteomes are herein reported for *H. antarcticus* (Staurozoa), *E. crocea* (Hydrozoa), and *T. coccinea* (Anthozoa) (Table 1 and Supplementary File S2). These data were combined with venom proteomes previously reported by us or obtained from the literature (Jaimes-Becerra et al. 2017) for the anthozoans *Acropora digitifera* (a zooxanthellate scleractinian coral) and *Anemonia viridis* (also zooxanthellate); the hydrozoans *Hydra magnipapillata* (freshwater polyp without medusa in the life cycle) and *O. sambaquiensis* (a hydromedusan); the scyphozoans *Aurelia aurita* and *Chrysaora lactea*; and the cubozoans *Chiropsalmus quadrumanus* and *Tamoya haplonema*. The distribution of the 32 protein families now revealed by proteome analyses of representatives of the major clades of cnidarians is shown in Fig. 1. 75% (24/32) of toxin protein families were shared between two or more cnidarian classes. Notably, Anthozoa contained seven of the eight unique toxin protein families. Inclusion of the first staurozoan data did not change previous understanding of cnidarian venom composition (Jaimes-Becerra et al. 2017), as no unique toxin protein families were identified in *H. antarcticus* (Fig. 1). Future work will determine if inclusion of myxozoans alters this perspective, and to address whether toxins in endocnidozoans (*Polypodium* + Myxozoa) are deployed differently than in free-living relatives.

To our knowledge use of the unsupervised clustering approach to analyze aligned sequence pairs has not been used previously to compare toxin composition between groups of venomous animals. Results of our analysis (Fig. 2) demonstrated that toxins group based on function rather than taxonomy of the venomous animal. Additionally, clustering and spread of individual data points demonstrated that despite the early divergence and morphological simplicity of cnidarians (Fig. 2A), toxin constituents of cnidarians venoms are variable and complex. Indeed, cnidarian toxins are more diverse than those of amphibians (Fig. 2B) and fish (Fig. 2C) and are comparable in complexity to those of insects (Fig. 2D), gastropods (Fig. 2E), and elapid snakes (which includes sea snakes, Fig. 2F). They appear to be not as complex as toxins of viperid snakes (Fig. 2G) or arachnids (spiders, scorpions, Fig. 2H). The complexity and diversification of cnidarian toxins reflect a long evolutionary history associated with lifestyles involving venoms for prey capture, competition for space (e.g., nematocysts in acrorhagi), and other defensive interactions in both benthic and pelagic habitats. Venom delivery in cnidarians is unique—nematocysts deployed across epithelial surfaces can be triggered to deliver venom collectively when prey or enemies make contact. Venom delivery in other animals tends to involve a point source, i.e., single or paired delivery devices situated anteriorly or posteriorly. The cnidarian delivery arrangement may facilitate immediate responses in morphologically simple animals that lack central nervous systems and hence have a limited ability to perceive threats and opportunities.

Nematocyst types and distribution are useful for cnidarian classification (Weill 1934; Östman 2000; Acuña et al. 2003) and phylogenetics (Marques and Collins 2004), and there is some evidence that nematocysts differing in size or shape might differ in venom composition (Macrander et al. 2016; Columbus-Shenkar et al. 2018). Alternatively, venom composition may alter according to requirements, for example prey type, as in snakes (Panagides et al. 2017). A recent quantitative proteomics study provides evidence against the scenario of venom variation with nematocyst type. Doonan et al. (2019) determined the variety and relative abundance of toxins present in enriched preparations of two nematocyst types with different penetrative abilities (microbasic mastigophore and microbasic eurytele capsules) isolated from tentacles of the medusa stage of the hydrozoan *O. sambaquiensis*. Venom composition of the nematocyst types was determined to be nearly identical, and there was little difference in toxin abundance. An emerging hypothesis from this study is that different nematocyst types deliver a single venom. Perhaps at least for some nematocyst types it is advantageous to produce a standard venom cocktail given the range of opportunities and threats that cnidarians may encounter. Morphologically more sophisticated animals with central nervous systems might be more prone to produce variable venoms that are suited to capture specific prey that can be perceived, tracked, and targeted. Evidence for tissue-specific toxicity (Kass-Simon and Scappaticci 2002; Fautin 2009) however,

Table 1 Potential venom toxins of *Haliclystus antarcticus*, *Ectopleura crocea*, and *Tubastraea coccinea* venoms

Peptide	**Protein family**	**UniProt accession number**	**Animal with closest similarity**
Haliclystus antarcticus			
DELTA-actitoxin-Ucs1a	Actinoporin	C9EIC7	*Urticina crassicornis*
A. superbus venom factor 1	Complement C3	Q0ZZJ6	*Austrelaps superbus*
Cobra venom factor	Complement C3	Q91132	*Naja kaouthia*
Conotoxin Lt9a	Conotoxin P superfamily	Q2I2P4	*Conus litteratus*
Turripeptide OL172	Conotoxin-like	P0DKP4	*Lophiotoma olangoensis*
Cysteine-rich venom protein natrin-1	CRISP	Q7T1K6	*Naja naja*
Venom allergen 5	CRISP	P35784	*Vespula germanica*
Hyaluronidase	Glycosyl hydrolase 56	Q08169	*Apis mellifera*
Hyaluronidase	Glycosyl hydrolase 56	P86687	*Polybia paulista*
Inactive hyaluronidase B	Glycosyl hydrolase 56	Q5D7H4	*Vespula vulgaris*
Toxin CfTX-2	Jellyfish toxin	A7L036	*Chironex fleckeri*
Kunitz-type serine protease inhibitor U1-aranetoxin-Av1a	Kunitz-type	Q8T3S7	*Araneus ventricosus*
M-zodatoxin-Lt4b	Latarcin	Q1ELU4	*Lachesana tarabaevi*
Alpha-latroinsectotoxin-Lt1a (Fragment)	Latrotoxin	Q02989	*Latrodectus tredecimguttatus*
Delta-latroinsectotoxin-Lt1a	Latrotoxin	Q25338	*Latrodectus tredecimguttatus*
Coagulation factor X-activating enzyme heavy chain	Metalloproteinase	Q7T046	*Macrovipera lebetina*
Metalloproteinase	Metalloproteinase	E9JGH2	*Echis carinatus sochureki*
Metalloproteinase 5	Metalloproteinase	F8S106	*Crotalus adamanteus*
Snake venom metalloproteinase (Type III) 6	Metalloproteinase	J3RY90	*Gloydius brevicaudus*
SVMP-CohPH-2	Metalloproteinase	T1DEB4	*Crotalus oreganus helleri*
Venom metalloproteinase 2	Metalloproteinase	B5AJT3	*Eulophus pennicornis*
Zinc metalloproteinase homolog-disintegrin albolatin	Metalloproteinase	P0C6B6	*Trimeresurus albolabris*
Zinc metalloproteinase-disintegrin-like atrolysin-A	Metalloproteinase	Q92043	*Crotalus atrox*
Phospholipase A1	Lipase	P0CH87	*Vespa crabro*
Beta-fibrinogenase stejnefibrase-2	Peptidase S1	Q8AY79	*Heloderma horridum horridum*
Serine protease sp-Eoc49	Peptidase S1	B5U6Y3	*Echis ocellatus*
Snake venom serine protease KN5	Peptidase S1	Q71QI4	*Trimeresurus stejnegeri*
Snake venom serine proteinase 14	Peptidase S1	J3SDW9	*Crotalus adamanteus*
Venom plasminogen activator GPV-PA	Peptidase S1	P0DJF5	*Trimeresurus albolabris*
Venom plasminogen activator TSV-PA	Peptidase S1	Q91516	*Trimeresurus stejnegeri*
Basic phospholipase A2 nigroxin B	Phospholipase A2	P81166	*Micrurus nigrocinctus*
Phospholipase D LbSicTox-betaIA1a	Phospholipase D	Q5YD76	*Loxosceles boneti*
Phospholipase D LiSicTox-alphaI-1 (Fragment)	Phospholipase D	P0C2L0	*Loxosceles intermedia*
Phospholipase D LruSicTox-alphaIC1a (Fragment)	Phospholipase D	C0JB03	*Loxosceles rufescens*
Phospholipase D StSicTox-betaIC1 (Fragment)	Phospholipase D	C0JB39	*Sicarius terrosus*
Phospholipase D StSicTox-betaIF1 (Fragment)	Phospholipase D	C0JB54	*Sicarius terrosus*
Snaclec mamushigin subunit alpha	Snaclec	Q9YGG9	*Gloydius blomhoffii*

(continued)

Table 1 Continued

	Haliclystus antarcticus		
Peptide	**Protein family**	**UniProt accession number**	**Animal with closest similarity**
Ectopleura crocea			
A. superbus venom factor 1	Complement C3	Q0ZZJ6	*Austrelaps superbus*
Cobra venom factor	Complement C3	Q91132	*Naja kaouthia*
Venom allergen 5	CRISP	P35780	*Polistes fuscatus*
Alpha-latrocrustotoxin-Lt1a	Latrotoxin	Q9XZC0	*Latrodectus tredecimguttatus*
Alpha-latroinsectotoxin-Lt1a	Latrotoxin	Q02989	*Latrodectus tredecimguttatus*
Alpha-latrotoxin-Lh1a	Latrotoxin	G0LXV8	*Latrodectus hasseltii*
Alpha-latrotoxin-Lhe1a	Latrotoxin	P0DJE3	*Latrodectus hesperus*
Venom metalloproteinase antarease TserMP_A	Metalloproteinase	P86392	*Tityus serrulatus*
Zinc metalloproteinase-disintegrin-like EoVMP2	Metalloproteinase	Q2UXQ5	*Echis ocellatus*
Zinc metalloproteinase-disintegrin-like VLAIP-B	Metalloproteinase	Q4VM07	*Macrovipera lebetina*
Bradykinin-potentiating and C-type natriuretic peptides	Natriuretic peptide	Q2PE51	*Crotalus durissus collilineatus*
C-type natriuretic peptide	Natriuretic peptide	Q09GK2	*Philodryas olfersii*
Natriuretic peptide	Natriuretic peptide	D1MZV3	*Rhabdophis tigrinus tigrinus*
Natriuretic peptide BM026	Natriuretic peptide	P0DMD5	*Bungarus multicinctus*
Phospholipase D LhSicTox-alphaIIIi	Phospholipase D	Q8I914	*Loxosceles laeta*
Phospholipase D LiSicTox-betaIIB1bx	Phospholipase D	COJB84	*Sicarius cf. damarensis*
Protein C activator	Peptidase S1	P09872	*Agkistrodon contortrix contortrix*
Serine protease harobin	Peptidase S1	Q5MCS0	*Hydrophis hardwickii*
Snake venom serine protease 2	Peptidase S1	Q9DF67	*Protobothrops jerdonii*
Venom prothrombin activator pseutarin-C catalytic subunit	Peptidase S1	Q56VR3	*Pseduonaja textilis*
Stonustoxin subunit alpha	SNTX/VTX	Q98989	*Synanceia horrida*
DELTA-alicitoxin-Pse2b	MAC-PF	P58912	*Phyllodiscus semoni*
Tubastraea coccinea			
Calglandulin	Calmodulin	adi_v1.03437	*Acropora digitifera*
Calglandulin	Calmodulin	adi_v1.01102	*Acropora digitifera*
Alpha-conotoxin	Conotoxin A superfamily	R4IKW2	*Conus ebraeus*
Conotoxin TsMLKM-02	Conotoxin M superfamily	Q9BPH4	*Conus tessulatus*
Venom allergen 5	CRISP	B2MVK7	*Rynchium brunneum*
L-amino-acid oxidase	Flavin monoamine oxidase	Q4JHE3	*Oxyuranus scutellatus scutellatus*
Hyaluronidase A	Glycosyl hydrolase 56	P49370	*Vespula vulgaris*
Alpha-latrotoxin-Lh1a	Latrotoxin	G0LXV8	*Latrodectus hasselti*
Metalloproteinase	Metalloproteinase	E9JG33	*Echis carinatus sochureki*
Zinc metalloproteinase-disintegrin-like ACLD	Metalloproteinase	O42138	*Agkistrodon contortrix laticinctus*
Ω-theraphotoxin-Hs1a	Neurotoxin 36	P68424	*Haplopelma schmidti*
Coagulation factor X isoform 2	Peptidase S1	Q1L658	*Pseudonaja textilis*
Peroxiredoxin-4	Peroxiredoxin	P0CV91	*Crotalus atrox*

(continued)

Table 1 Continued

	Haliclystus antarcticus		
Peptide	**Protein family**	**UniProt accession number**	**Animal with closest similarity**
Basic phospholipase A2 pseudexin A chain	Phospholipase A2	P20258	*Pseudechis porphyriacus*
Phospholipase D SpaSicTox-betaIF1	Phospholipase D	C0JB52	*Sicarius patagonicus*
Waprin-Phi1	Snake Waprin	A7X4K1	*Philodryas olfersii*
Stonustoxin subunit-α	SNTX/VTX	Q98989	*Synanceia horrida*
Three finger toxin	Snake three finger	A0A098LYI1	*Pantherophis guttatus*

Putative toxins were identified by homology of peptide sequences obtained from *de novo* sequencing of unique MS/MS events with known animal venom toxins. Venomous animals and their toxins with closest sequence similarity are given together with the corresponding UniProt accession number.

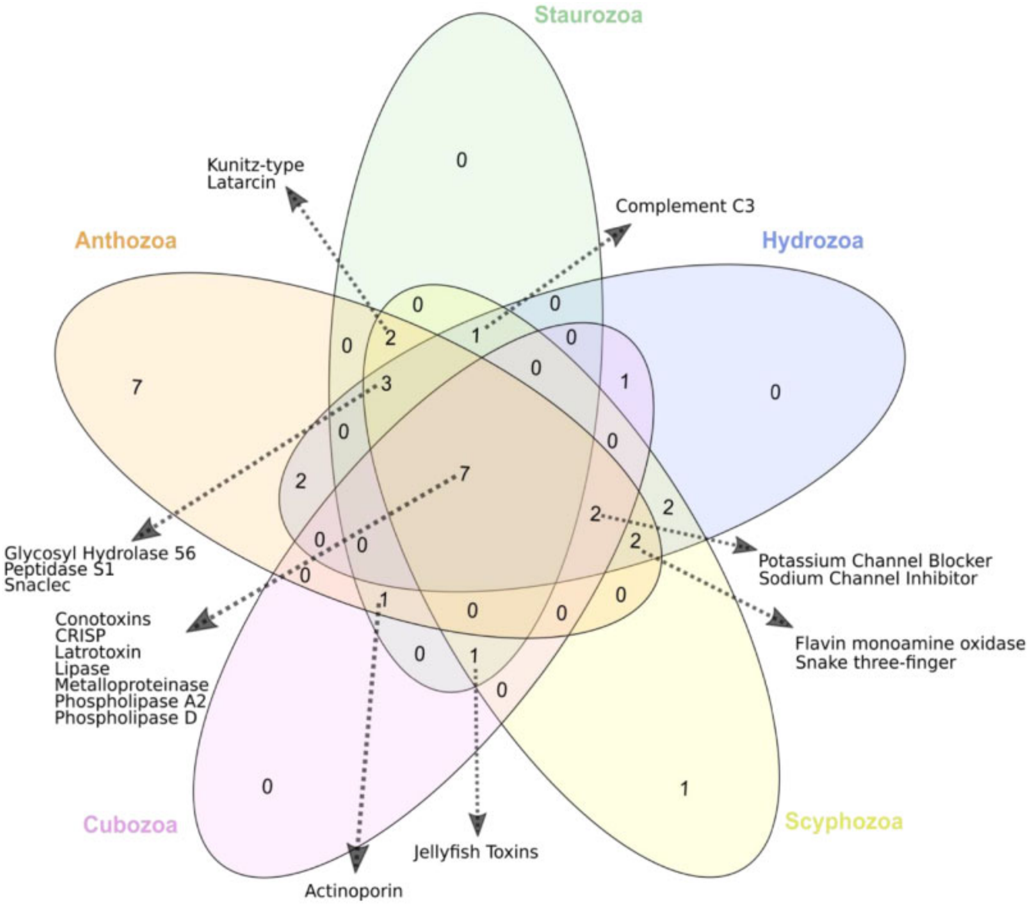

Fig. 1 Comparison of the putative venom proteomes from the discharged nematocysts of 11 cnidarians. The Venn diagram shows the number of toxin protein families shared among the major free-living cnidarian classes. Overall, 75% of the toxin protein families were shared by two or more classes. Only 25% (8/32) of the toxin protein families were unique to a single class, with 88% (7/8) unique to the Anthozoa.

suggests that cnidarians may vary venom content according to variation in activities associated with internal and external epithelial surfaces.

Conclusions and closing remarks

Further scrutiny of cnidarian venom diversity, variation among nematocyst types and distributions in body regions may provide insights into venom evolution within cnidarians and other metazoans. Results to date suggest little variation in venom composition between nematocyst types or according to phylogeny, although the abundance of some toxins may vary. How toxin abundances can be "tweaked" remains elusive, and it is unclear if shifts in toxin abundance influence behavior or whether behavior

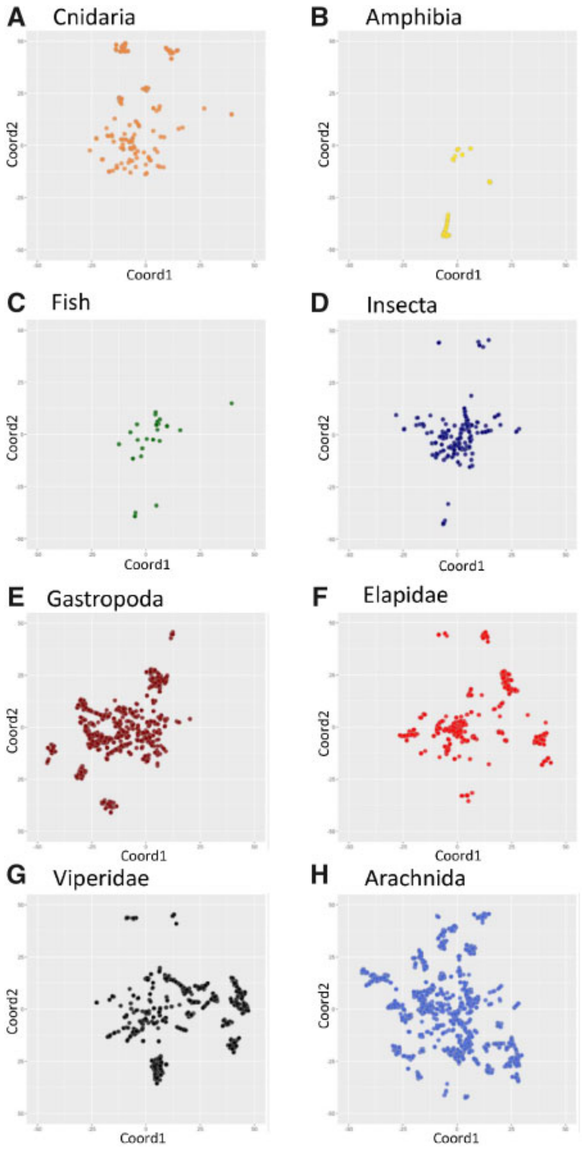

Fig. 2 Cluster free comparison of venom toxin composition between major phyla of venomous animals. The comparison was made using t-SNE clustering of over 6000 animal venom toxins deposited in the UniProtKB/SwissProt-ToxProt based on a blastp-generated distance matrix. Toxins with similar sequence can be reduced to single data points. Data points that group closely are indicative of toxins with similar predicted biological functions. The greater the spread of data points the more broad spectrum the venom of a particular taxon is forecast to possess. Despite the early divergence of **A**) cnidarians, their venoms appear more complex than **B**) amphibians and **C**) fish, and are just as diverse as **D**) insects, **E**) gastropods, and **F**) elapid snakes; but not as complicated as the venom of **G**) vipers and **H**) arachnids.

triggers regulation of toxin expression at the gene, transcript, or protein level.

Further investigation of cnidarian venoms could lead to discovery of novel therapeutic peptides of pharmaceutical interest since LC/MS/MS data that we and others have acquired also contain many high-quality MS/MS spectra that remain unassigned (Madio et al. 2017). Future research is required to integrate *de-novo* peptide sequencing with homology matching to other datasets in order to assign sequences to tandem mass spectra that at present are routinely discarded. Identifying venom diversity is also challenging because of constraints in assigning biological function to sequence data solely using homology searching without experimental validation.

Acknowledgments

We are grateful to Karla Paresque (Universidade Federal de Alagoas), Lucília Miranda (Universidade Federal de Minas Gerais), Luiza Sandoval-Perin (Universidade de São Paulo), and Marcelo Visentini Kitahara (Universidade Federal de São Paulo) for providing specimens. The Centre for Marine Biology of the University of São Paulo (CEBIMar-USP) hosted and supported most of the field work. Technical support for proteomics was provided by Steven Lynham and Malcolm Ward at the Centre of Excellence for Mass Spectrometry King's College London.

Funding

Financial support for this work was received from the Leverhulme Trust [grant number RPG-2016-037]. Funds were also received from DEDE, DNNSB, DPCB of SICB, and from the American Microscopical Society. Additional funding from Brazil came from CNPq [grant number 309995/2017-5], CAPES [grant number 236.507.518-52], FAPESP [grant number 2011/50242-5], and USP [grant number 13.1.1502.9.8].

Supplementary data

Supplementary data are available at *ICB* online.

References

Acuña FH, Excoffon AC, Zamponi MO, Ricci L. 2003. Importance of nematocysts in taxonomy of acontiarian sea anemones (Cnidaria, Actiniaria): a statistical comparative study. Zool Anz 242:75–81.

Badré S. 2014. Bioactive toxins from stinging jellyfish. Toxicon 91:114–25.

Balasubramanian PG, Beckmann A, Warnken U, Schnölzer M, Schüler A, Bornberg-Bauer E, Holstein TW, Özbek S. 2012. Proteome of *Hydra* nematocyst. J Biol Chem 287:9672–81.

Brinkman DL, Jia X, Potriquet J, Kumar D, Dash D, Kvaskoff D, Mulvenna J. 2015. Transcriptome and venom proteome of the box jellyfish *Chironex fleckeri.* BMC Genomics 16:1–15.

Camacho C, Coulouris G, Avagyan V, Ning M, Papadopoulos J, Bealer K, Madden TL. 2009. BLAST+: architecture and applications. BMC Bioinformatics 10:1–9.

Church JE, Hodgson WC. 2002. The pharmacological activity of fish venoms. Toxicon 40:1083–93.

Columbus-Shenkar YY, Sachkova MY, Macrander J, Fridrich A, Modepalli V, Reitzel AM, Sunagar K, Moran Y. 2018. Dynamics of venom composition across a complex life cycle. eLIFE 7:e35014.

De Graaf DC, Aerts M, Danneels E, Devreese B. 2009. Bee, wasp and ant venomics pave the way for a component-resolved diagnosis of sting allergy. J Proteomics 72:145–54.

Doonan LB, Lynham S, Quinlan C, Ibiji SC, Winter CE, Padilla G, Jaimes-Becerra A, Morandini AC, Marques AC, Long PF. Forthcoming 2019. Venom composition does not vary greatly between different nematocyst types isolated from the primary tentacles of *Olindias sambaquiensis* (Cnidaria: Hydrozoa). Biol Bull.

Fautin DG. 2009. Structural diversity, systematics, and evolution of Cnidae. Toxicon 54:1054–64.

Frickey T, Lupas A. 2004. CLANS: a Java application for visualizing protein families based on pairwise similarity. Bioinformatics 20:3702–4.

Fry BG, Roelants K, Champagne DE, Scheib H, Tyndall JD, King GF, Nevalainen TJ, Norman J, Lewis RJ, Norton RS, et al. 2009. The toxicogenomic multiverse: convergent recruitment of proteins into animal venoms. Annu Rev Genomics Hum Genet 10:483–511.

Gacesa R, Barlow D, Long PF. 2016. Machine learning can differentiate venom toxins from other proteins having non-toxic physiological functions. PeerJ Comp Sci 2:e90.

Heberle H, Meirelles GV, da Silva FR, Telles GP, Minghim R. 2015. InteractiVenn: a web-based tool for the analysis of sets through Venn diagrams. BMC Bioinformatics 16:169.

Huang C, Morlighem JR, Zhou H, Lima ÉP, Gomes PB, Cai J, Lou I, Pérez CD, Lee SM, Rádis-Baptista G. 2016. The transcriptome of the zoanthid *Protopalythoa variabilis* (Cnidaria, Anthozoa) predicts a basal repertoire of toxin-like and venom-auxiliary polypeptides. Genome Biol Evol 8:3045–64.

Jaimes-Becerra A, Chung R, Morandini A, Weston AJ, Padilla G, Gacesa R, Ward M, Long PF, Marques AC. 2017. Comparative proteomics reveals recruitment patterns of some protein families in the venoms of Cnidaria. Toxicon 137:19–26.

Jungo F, Bougueleret L, Xenarios I, Poux S. 2012. The UniProtKB/Swiss-Prot Tox-Prot program: a central hub of integrated venom protein data. Toxicon 60:551–5.

Kass-Simon G, Scappaticci J. 2002. The behavioral and developmental physiology of nematocysts. Can J Zool 80:1772–94.

Li R, Yu H, Xue W, Yue Y, Liu S, Xing R, Li P. 2014. Jellyfish venomics and venom gland transcriptomics analysis of *Stomolophus meleagris* to reveal the toxins associated with sting. J Proteomics 106:17–29.

Li R, Yu H, Yue Y, Liu S, Xing R, Chen X, Li P. 2016. Combined proteomics and transcriptomics identifies sting-related toxins of jellyfish *Cyanea nozakii*. J Proteomics 148:57–64.

Macrander J, Brugler MR, Daly M. 2015. A RNA-seq approach to identify putative toxins from acrorhagi in aggressive and non-aggressive *Anthopleura elegantissima* polyps. BMC Genomics 16:1–19.

Macrander J, Broe M, Daly M. 2016. Tissue-specific venom composition and differential gene expression in sea anemones. Genome Biol Evol 8:2358–75.

Madio B, Undheim EAB, King GF. 2017. Revisiting venom of the sea anemone *Stichodactyla haddoni*: omics techniques reveal the complete toxin arsenal of a well-studied sea anemone genus. J Proteomics 166:83–92.

Mariottini GL, Bonello G, Giacco E, Pane L. 2015. Neurotoxic and neuroactive compounds from Cnidaria: five decades of research . . . . and more. Cent Nerv Syst Agents Med Chem 15:74–80.

Marques AC, Collins AG. 2004. Cladistic analysis of Medusozoa and cnidarian evolution. Invertebr Biol 123:23–42.

Nelsen DR, Nisani Z, Cooper AM, Fox GA, Gren ECK, Corbit AG, Hayes WK. 2014. Poisons, toxins, and venoms: redefining and classifying toxic biological secretions and the organisms that employ them. Biol Rev 89:450–65.

Östman C. 2000. A guideline to nematocyst nomenclature and classification, and some notes on the systematic value of nematocysts. Sci Mar 64:31–46.

Panagides N, Jackson TN, Ikonomopoulou MP, Arbuckle K, Pretzler R, Yang DC, Ali SA, Koludarov I, Dobson J, Sanker B, et al. 2017. How the cobra got its flesh-eating venom: cytotoxicity as a defensive innovation and its co-evolution with hooding, aposematic marking, and spitting. Toxins (Basel) 9:E103.

Peiren N, Vanrobaeys F, de Graaf DC, Devreese B, van Beeumen J, Jacobs FJ. 2005. The protein composition of honeybee venom reconsidered by a proteomic approach. Biochim Biophys Acta 1752:1–5.

Podobnik M, Anderluh G. 2017. Pore-forming toxins in Cnidaria. Semin Cell Dev Biol 72:133–41.

Ponce D, Brinkman DL, Potriquet J, Mulvenna J. 2016. Tentacle transcriptome and venom proteome of the Pacific sea nettle, *Chrysaora fuscescens* (Cnidaria: Scyphozoa). Toxins (Basal) 8:102.

Rachamim T, Morgenstern D, Aharonovich D, Brekhman V, Lotan T, Sher D. 2015. The dynamically evolving nematocyst content of an anthozoan, a scyphozoan, and a hydrozoan. Mol Biol Evol 32:740–53.

Starcevic A, Long PF. 2013. Diversification of animal venom peptides—were jellyfish amongst the first combinatorial chemists? ChemBioChem 14:1407–9.

Šuput D. 2009. *In vivo* effects of cnidarian toxins and venoms. Toxicon 54:1190–200.

van der Maaten L, Hinton G. 2008. Visualizing data using t-SNE. Ann Oper Res 9:2579–605.

Weill R. 1934. Contribution à l'étude des cnidaires et de leurs nématocystes. Trav St Zool Wimereux 10–11:1–701.

Weston AJ, Dunlap WC, Shick JM, Klueter A, Iglic K, Vukelic A, Starcevic A, Ward M, Wells ML, Trick CG, Long PF. 2012. A profile of an endosymbiont-enriched fraction of the coral *Stylophora pistillata* reveals proteins relevant to microbial–host interactions. Mol Cell Proteomics 11:M111.015487.

Weston AJ, Chung R, Dunlap WC, Morandini AC, Marques AC, Moura-da-Silva AM, Ward M, Padilla G, da Silva LF, Andreakis N, et al. 2013. Proteomic characterization of toxins isolated from nematocysts of the South Atlantic jellyfish *Olindias sambaquiensis*. Toxicon 71:11–7.